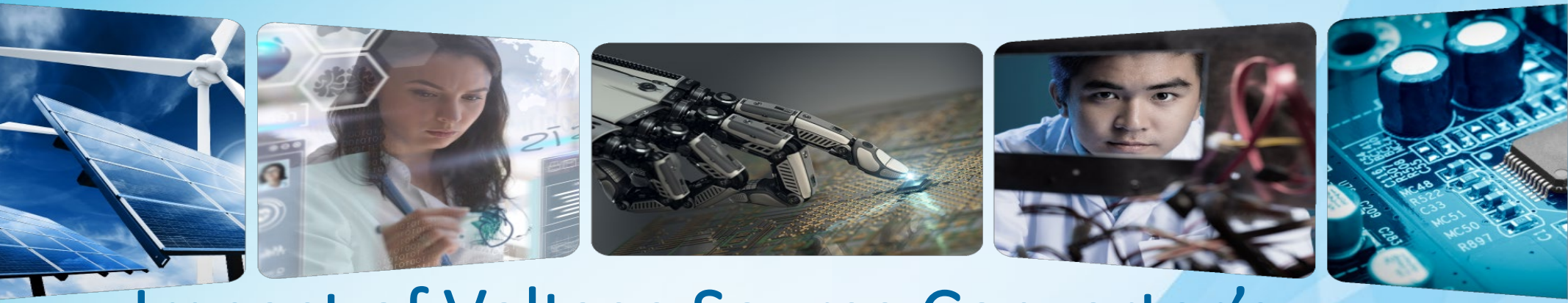

Impact of Voltage Source Converter's Control on the Power System Small-Signal Voltage Stability

By ir. Yin Sun, Senior Researcher

Power and Renewables Program, DNV GL Group Technology Research

IEEE

Agenda

- Background
- Voltage-Source-Converter Modelling
- Impedance-based Stability Criteria
- Experimental Results
- Summary

Energy Transition

- **Economic growth:** Gross World Product (GWP) will grow 130% by 2050 (from 2015)

  By mid-century, even today's rapidly growing emerging economies will experience significantly slower growth as their economies de-industrialize and become more service orientated

- **Population**: projected global population in 2050 of 9.2 billion

  This is 6% lower than the latest (2017) UN median forecast, and reflects our view that rapid urbanization and rising education levels will lead to more sharply declining fertility levels

- **Learning Curves:** forecast average cost reduction per doubling of installed capacity - wind 16% solar PV 16%

  Non-renewable energy sources have shown impressive cost cuts in recent years, but installed capacity of such sources will not expand at the same rate as renewable sources; hence a lower cost-learning curve effect

- **Global energy intensity:** decline in units of energy required per units of GDP will improve from an historical average 1.4%/yr to 2.5%/yr

  This is linked to many technology and usage efficiency gains, but is mainly the result of the rapid electrification of the world's energy system, driven by efficient renewables

Power Electronics – Underpinning Technology

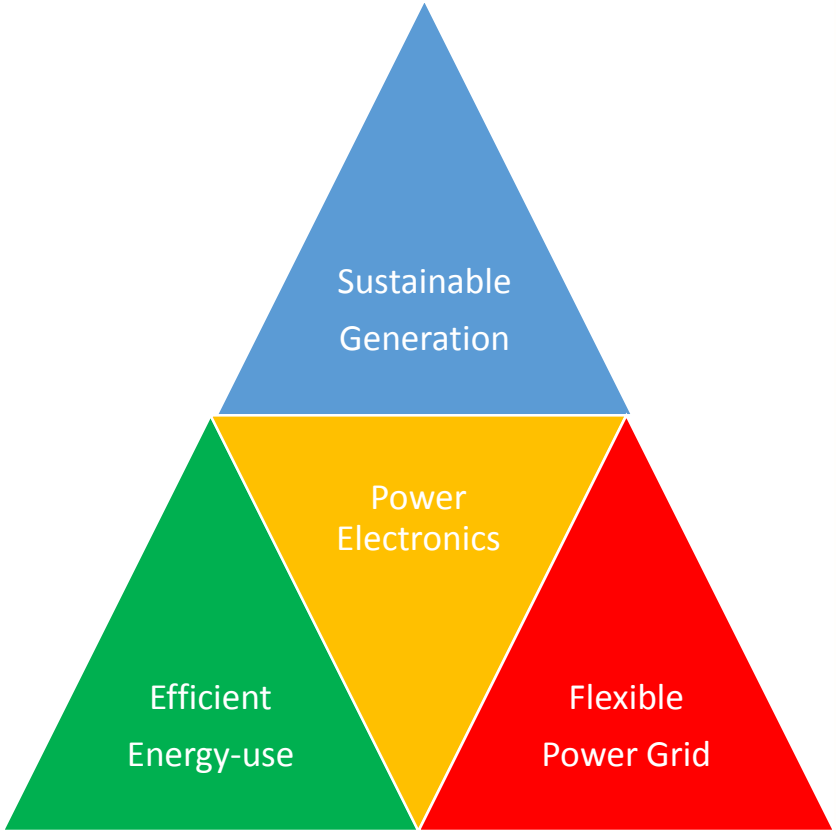

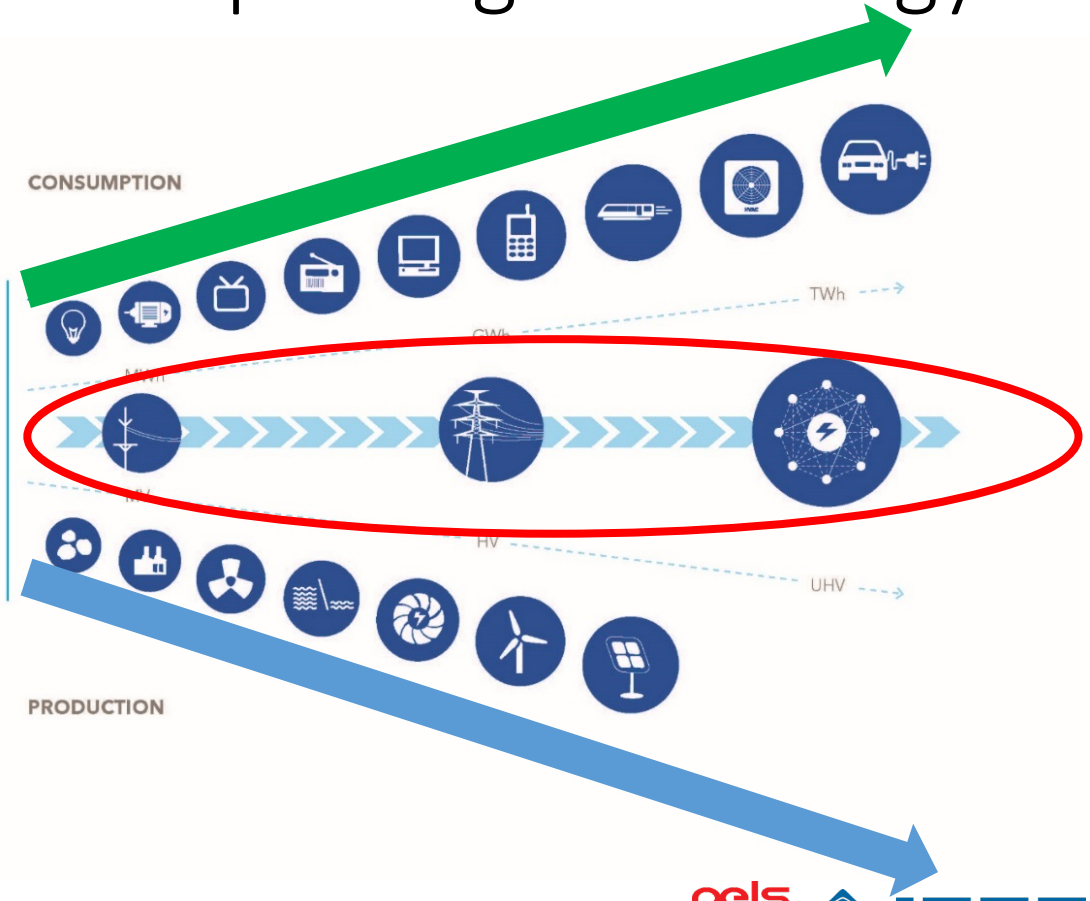

A Power Electronics Dominant Grid

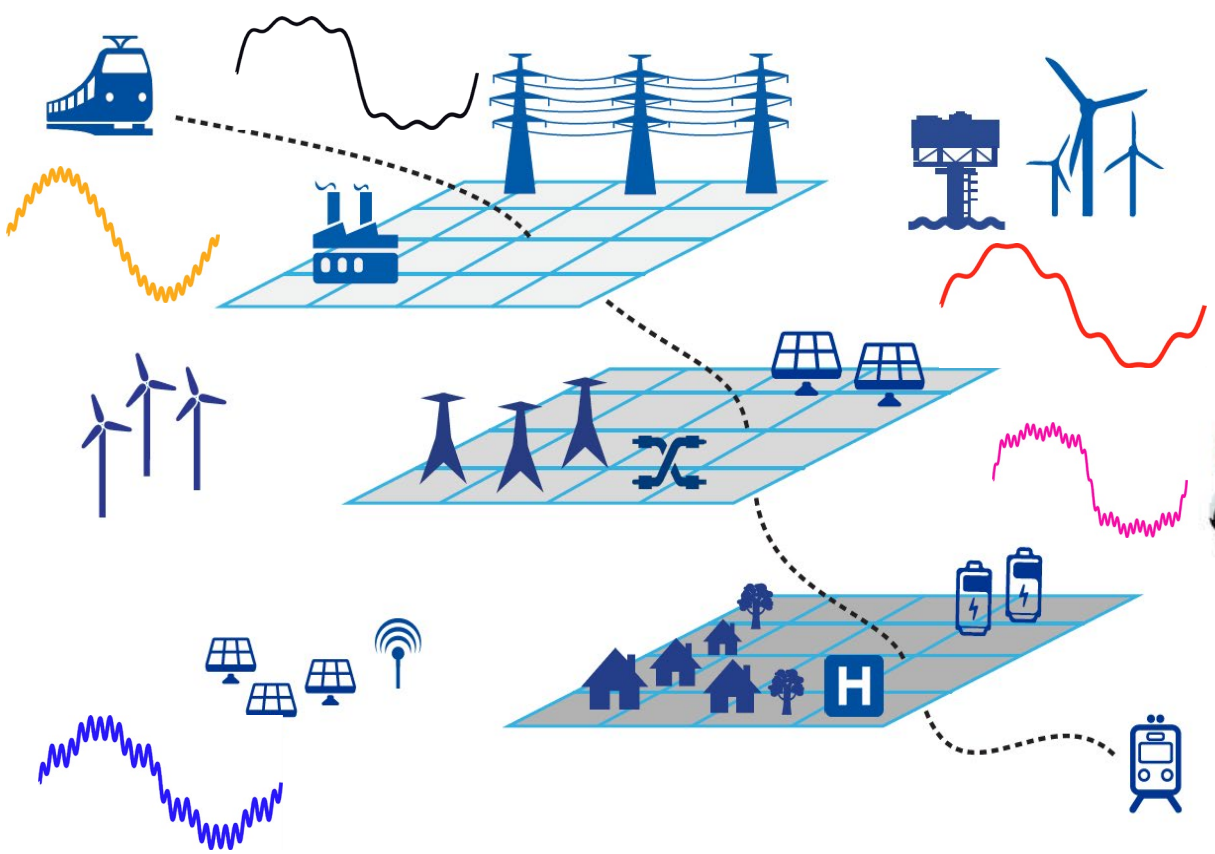

Challenges and Issues

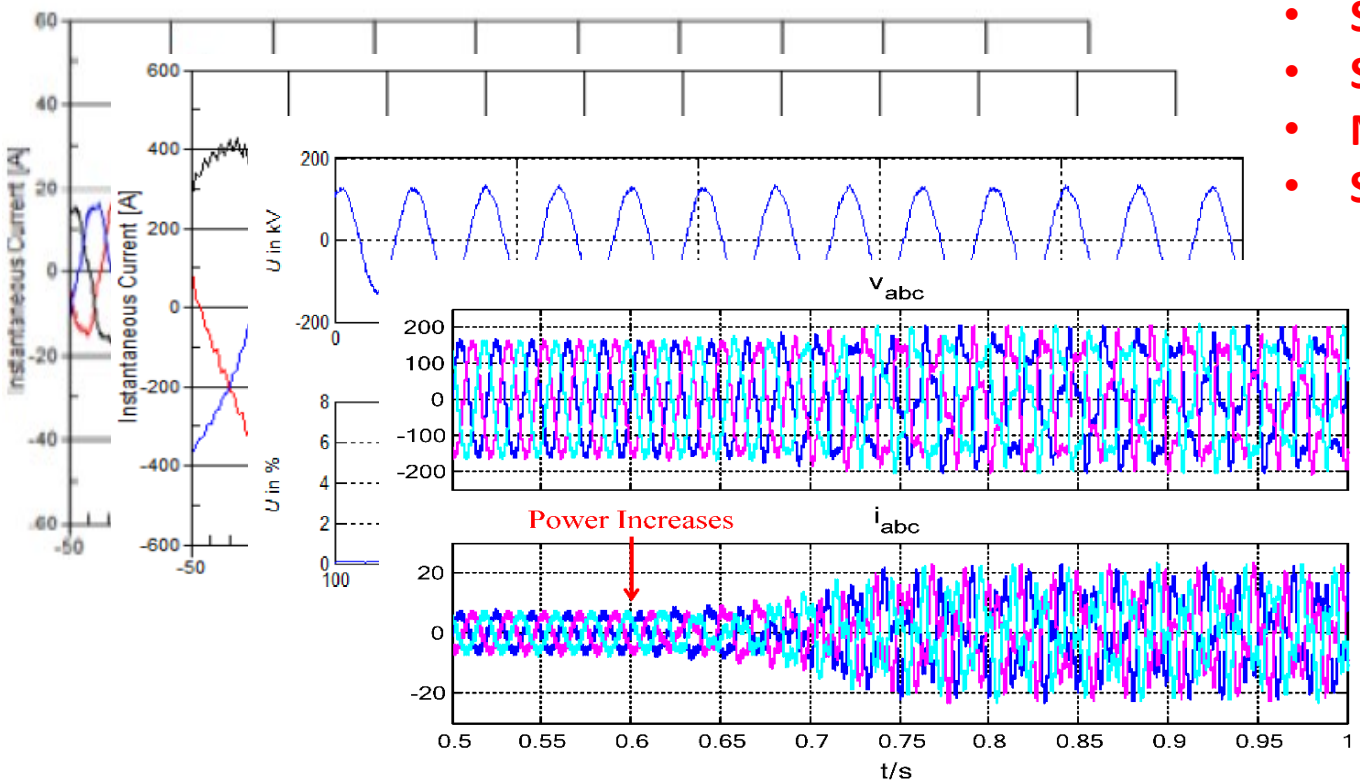

- **Subsynchronous oscillation**
- **Supersynchronous oscillation**
- **Non-characteristic harmonics**
- **Setpoint dependent**

Source: C. Li, "Unstable Operation of Photovoltaic Inverter from Field Experiences," IEEE Trans. Power Deliv., vol. 8977, no. c, pp. 1–1, 2017.

J. Sun, C. Buchhagen, and M. Greve, "Impedance Modeling and Simulation of Wind Turbines for Power System Harmonic Analysis", Session 3A-1, Wind Integration Workshop 2017, Berlin, Germany.

Grid-connected VSC applications

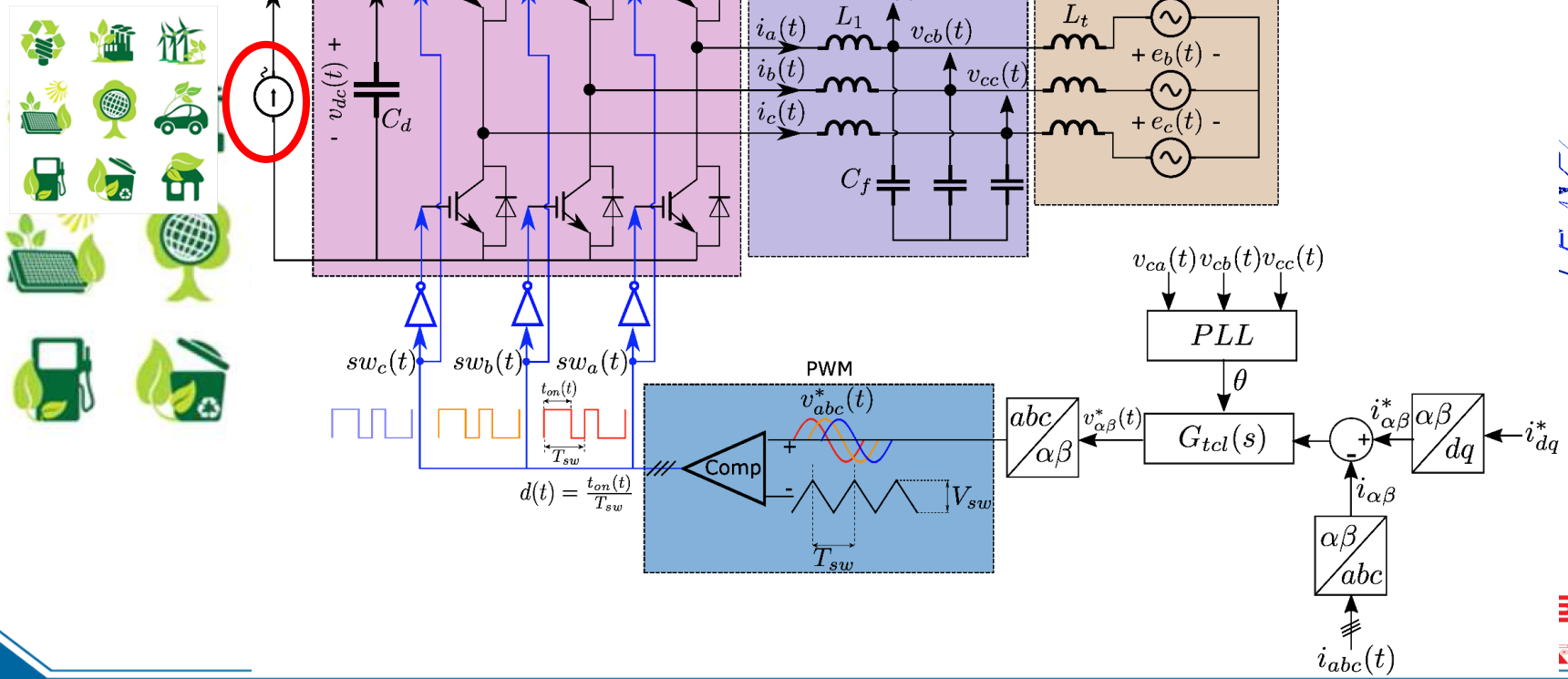

Modelling of Voltage-Source-Converter (1)

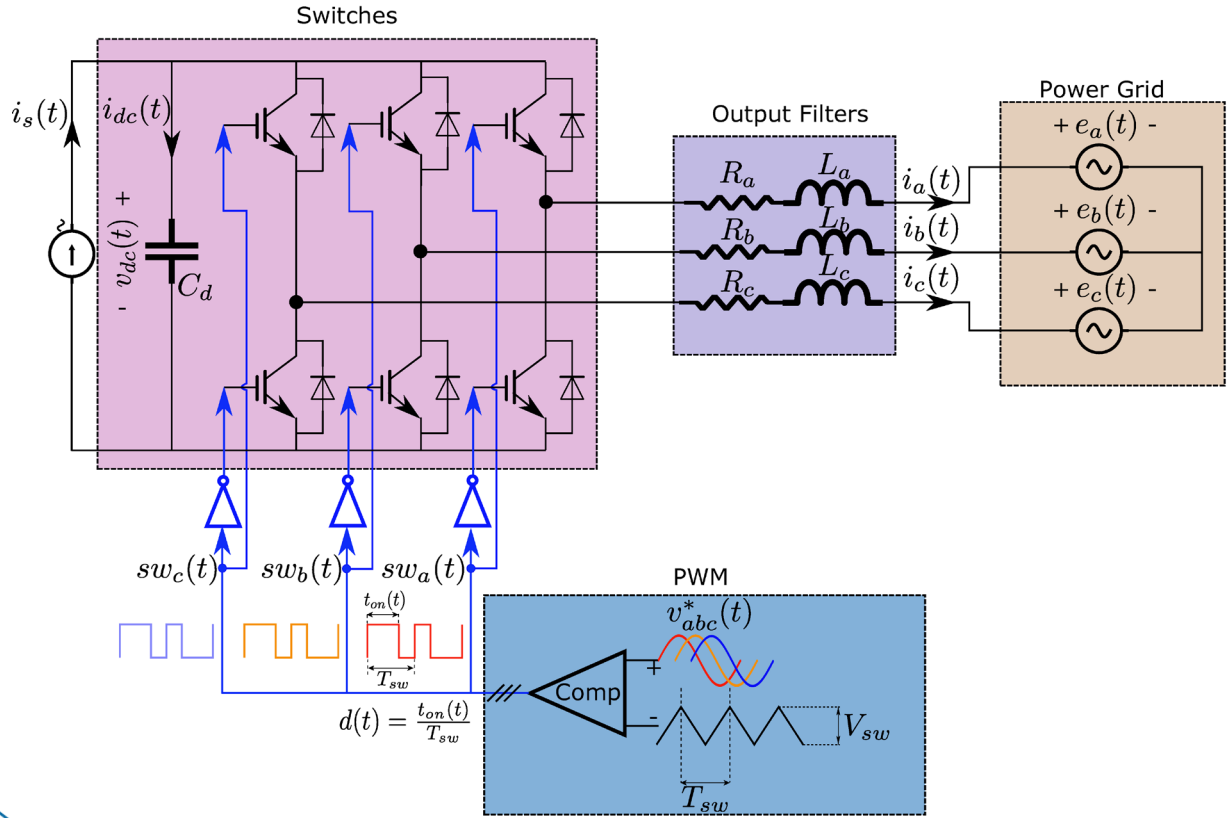

$$L_a \frac{di_a(t)}{dt} + i_a(t)R_a + e_a(t) - sw_a(t)v_{dc}(t) = \frac{1}{3}\sum_{x=a,b,c} sw_x(t)$$

$$L_b \frac{di_b(t)}{dt} + i_b(t)R_b + e_b(t) - sw_b(t)v_{dc}(t) = \frac{1}{3}\sum_{x=a,b,c} sw_x(t)$$

$$L_c \frac{di_c(t)}{dt} + i_c(t)R_c + e_c(t) - sw_c(t)v_{dc}(t) = \frac{1}{3}\sum_{x=a,b,c} sw_x(t)$$

$$\dot{x}(t) = A(t)x(t) + Bu(t)$$

$$y(t) = Cx(t)$$

$$\dot{x}(t) \triangleq \frac{\mathrm{d}}{\mathrm{d}t}\begin{bmatrix} i_a(t) \\ i_b(t) \\ i_c(t) \\ v_{dc}(t) \end{bmatrix} \qquad u(t) \triangleq \begin{bmatrix} e_a(t) \\ e_b(t) \\ e_c(t) \\ i_s(t) \end{bmatrix}$$

Modelling of Voltage-Source-Converter (2)

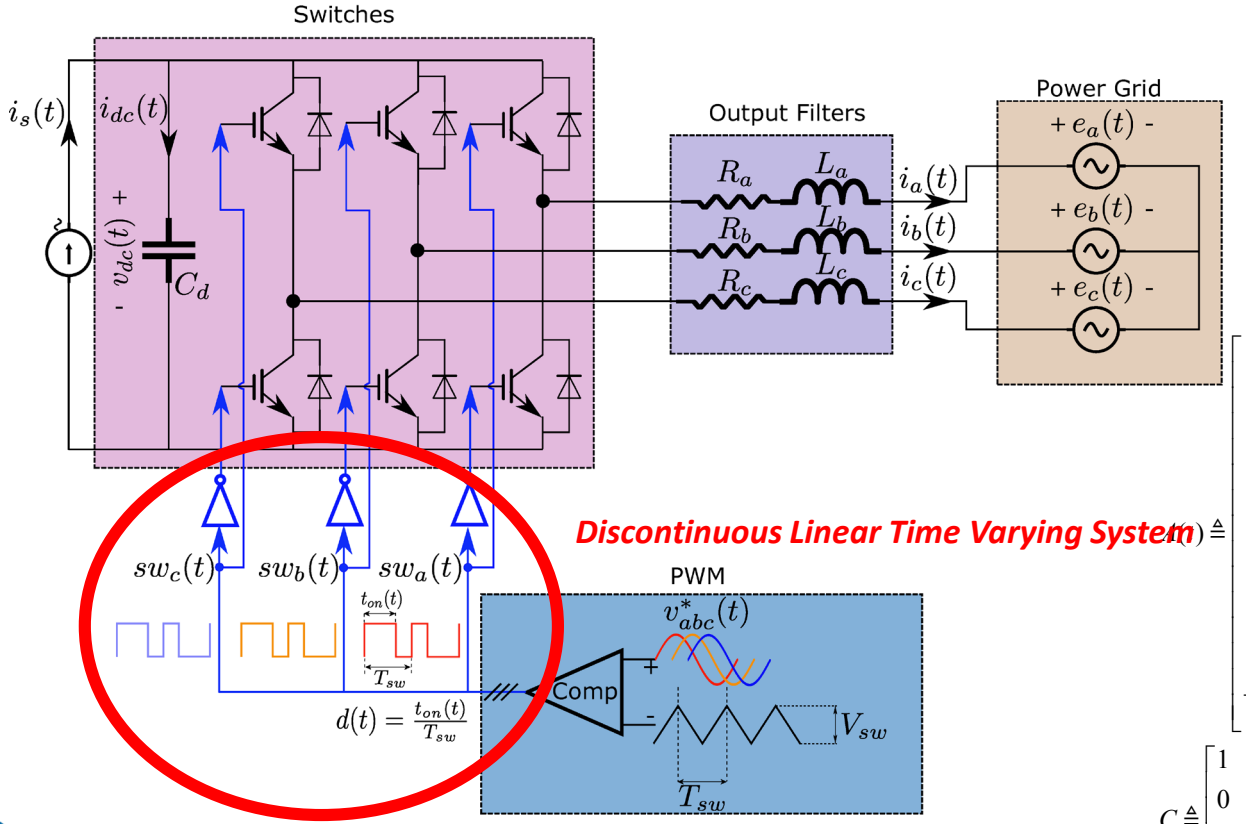

Discontinuous Linear Time Varying System

$$\dot{x}(t) = A(t)x(t) + Bu(t)$$
$$y(t) = Cx(t)$$

$$\dot{x}(t) \triangleq \frac{\mathrm{d}}{\mathrm{d}t}\begin{bmatrix} i_a(t) \\ i_b(t) \\ i_c(t) \\ v_{dc}(t) \end{bmatrix} \qquad u(t) \triangleq \begin{bmatrix} e_a(t) \\ e_b(t) \\ e_c(t) \\ i_s(t) \end{bmatrix}$$

$$A(t) \triangleq \begin{bmatrix} -\frac{R}{L} & 0 & 0 & \frac{sw_a(t) + \frac{1}{3}\sum_{x=a,b,c} sw_x(t)}{L} \\ 0 & -\frac{R}{L} & 0 & \frac{sw_b(t) + \frac{1}{3}\sum_{x=a,b,c} sw_x(t)}{L} \\ 0 & 0 & -\frac{R}{L} & \frac{sw_c(t) + \frac{1}{3}\sum_{x=a,b,c} sw_x(t)}{L} \\ -\frac{sw_a(t)}{C_d} & -\frac{sw_b(t)}{C_d} & -\frac{sw_c(t)}{C_d} & 0 \end{bmatrix} \qquad B \triangleq \begin{bmatrix} -\frac{1}{L} & 0 & 0 & 0 \\ 0 & -\frac{1}{L} & 0 & 0 \\ 0 & 0 & -\frac{1}{L} & 0 \\ 0 & 0 & 0 & \frac{1}{C_d} \end{bmatrix}$$

$$C \triangleq \begin{bmatrix} 1 & 0 & 0 & 0 \\ 0 & 1 & 0 & 0 \\ 0 & 0 & 1 & 0 \\ 0 & 0 & 0 & 1 \end{bmatrix}$$

Modelling of Voltage-Source-Converter (3)

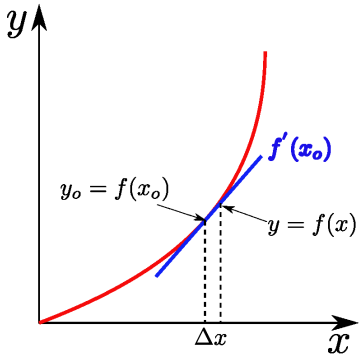

Linearization by Taylor's series

Coordinates Transformation

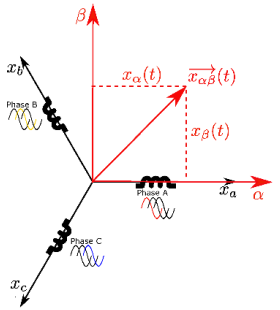

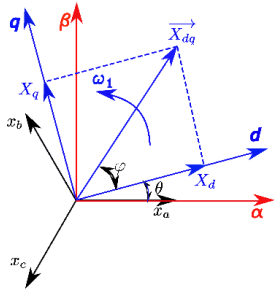

Averaging Method

Linear Time Invariant

Constant DC Link Voltage

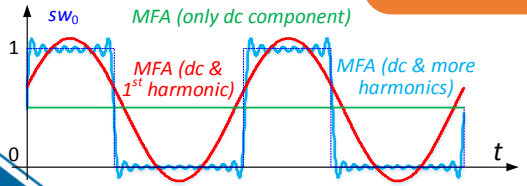

Modelling of Voltage-Source-Converter (4)

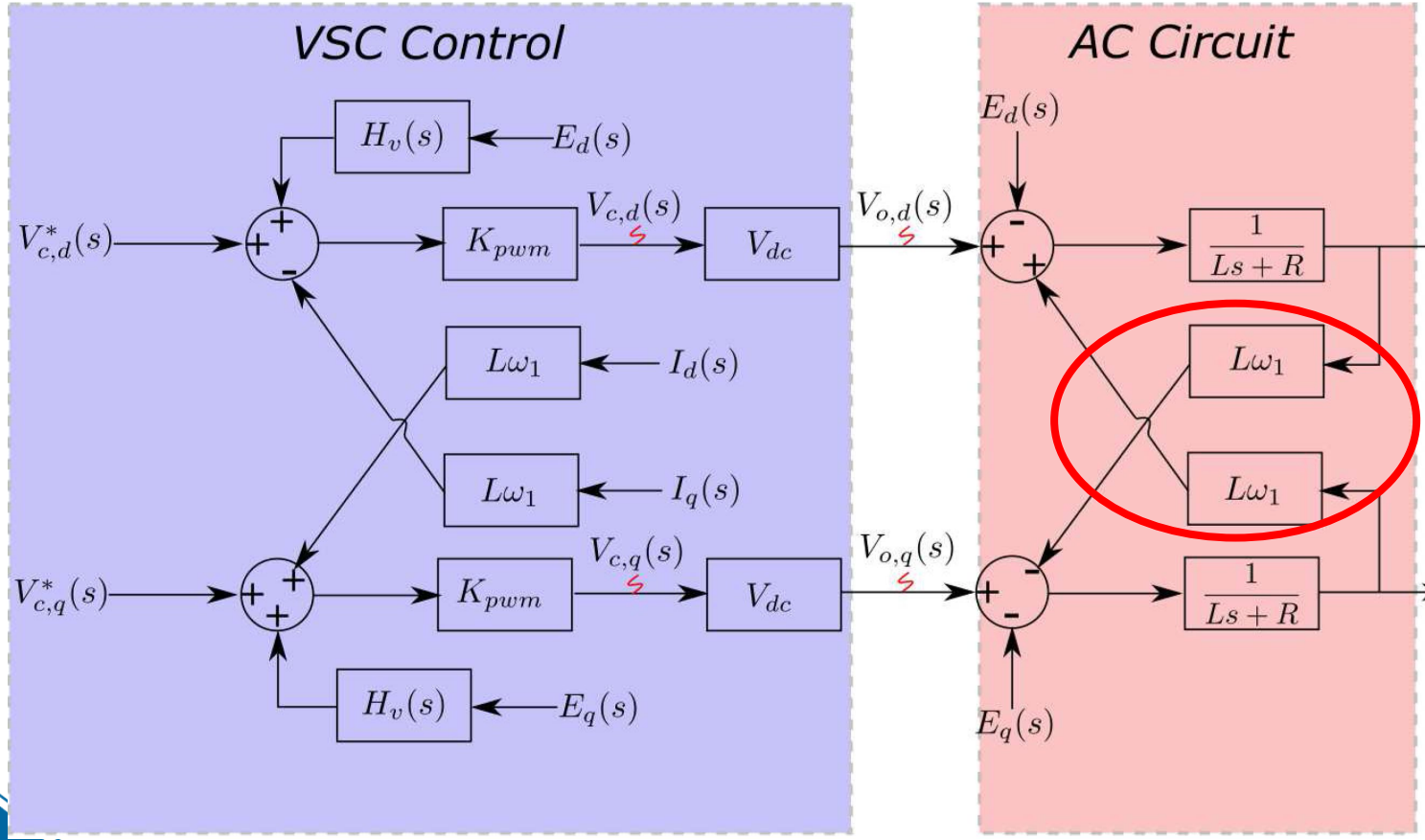

$$L\frac{\mathrm{d}\vec{i}_{dq}(t)e^{j\theta}}{\mathrm{d}t} = L\frac{\mathrm{d}\vec{i}_{dq}(t)}{\mathrm{d}t}e^{j\theta} + L\frac{\mathrm{d}e^{j\theta}}{\mathrm{d}t}\vec{i}_{dq}(t)$$
$$= L\frac{\mathrm{d}\vec{i}_{dq}(t)}{\mathrm{d}t}e^{j\theta} + jL\frac{\mathrm{d}\theta}{\mathrm{d}t}\vec{i}_{dq}(t)e^{j\theta}$$
$$= L\frac{\mathrm{d}\vec{i}_{dq}(t)}{\mathrm{d}t}e^{j\theta} + jL\omega_1\vec{i}_{dq}(t)e^{j\theta}$$

Impedance-based Stability Criteria

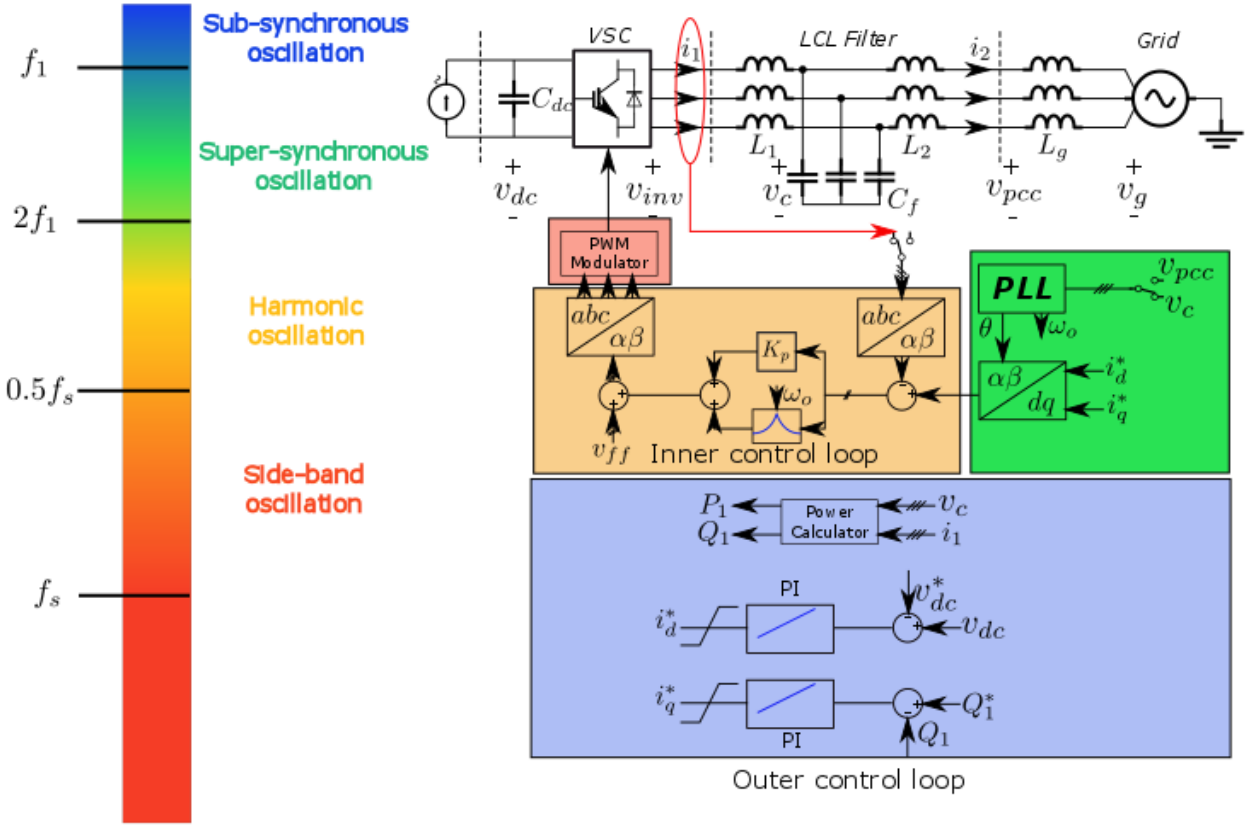

Nyquist Stability Criterion

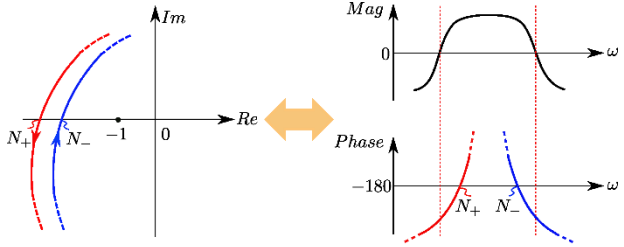

Impedance-based Stability Criterion

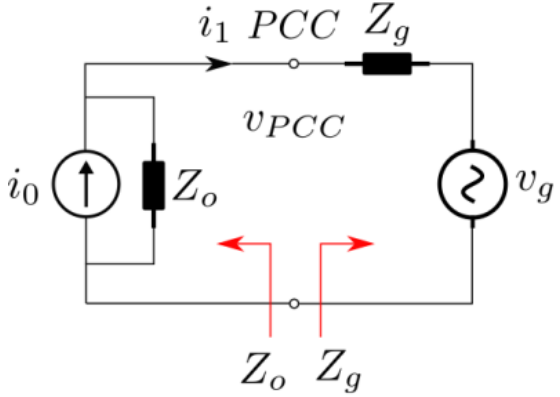

dq-frame input admittance matrix

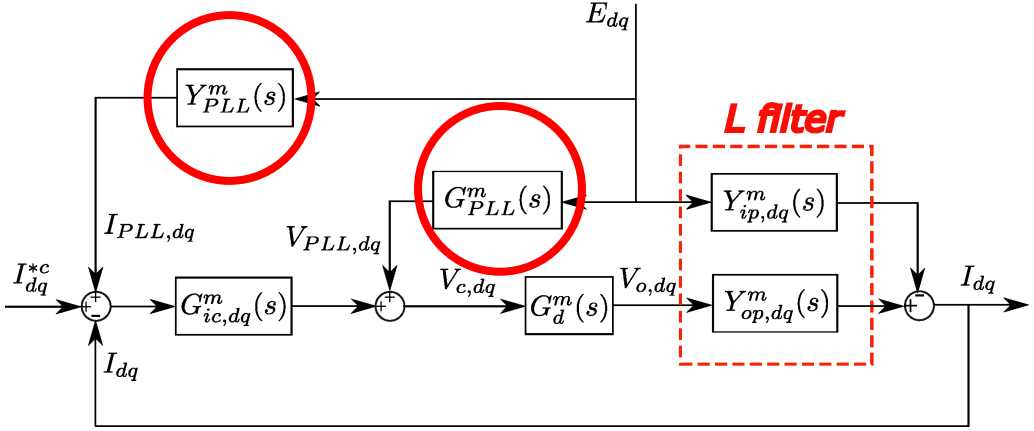

$$\begin{bmatrix} I_{PLL,d} \\ I_{PLL,q} \end{bmatrix} = \underbrace{\begin{bmatrix} 0 & -H_{pll}(s)I_{1q} \\ 0 & H_{pll}(s)I_{1d} \end{bmatrix}}_{Y^m_{PLL}(s)} \begin{bmatrix} E_d \\ E_q \end{bmatrix} \quad \begin{bmatrix} V_{PLL,d} \\ V_{PLL,q} \end{bmatrix} = \underbrace{\begin{bmatrix} 0 & -H_{pll}(s)V_{1cq} \\ 0 & H_{pll}(s)V_{1cd} \end{bmatrix}}_{G^m_{PLL}(s)} \begin{bmatrix} E_d \\ E_q \end{bmatrix}$$

$$\begin{bmatrix} \Delta I_d \\ \Delta I_q \end{bmatrix} = G^m_{tcl,dq}(s) \underbrace{\begin{bmatrix} \Delta I^{*c}_d \\ \Delta I^{*c}_q \end{bmatrix}}_{\Delta \vec{\mathbf{I}}^{*c}_{dq}} - \underbrace{\left(\overbrace{-G^m_{tcl,dq}(s)Y^m_{PLL}(s)}^{PLL-dynamics} + Y^m_{to,dq} \right)}_{Y^m_{tcl}(s)} \begin{bmatrix} \Delta E_d \\ \Delta E_q \end{bmatrix}$$

$$\begin{bmatrix} I_d \\ I_q \end{bmatrix} = \underbrace{\begin{bmatrix} Y_{dd}(s) & Y_{dq}(s) \\ Y_{qd}(s) & Y_{qq}(s) \end{bmatrix}}_{Y^m_{tcl,dq}} \begin{bmatrix} E_d \\ E_q \end{bmatrix}$$

Experimental Results – Laboratory Setup

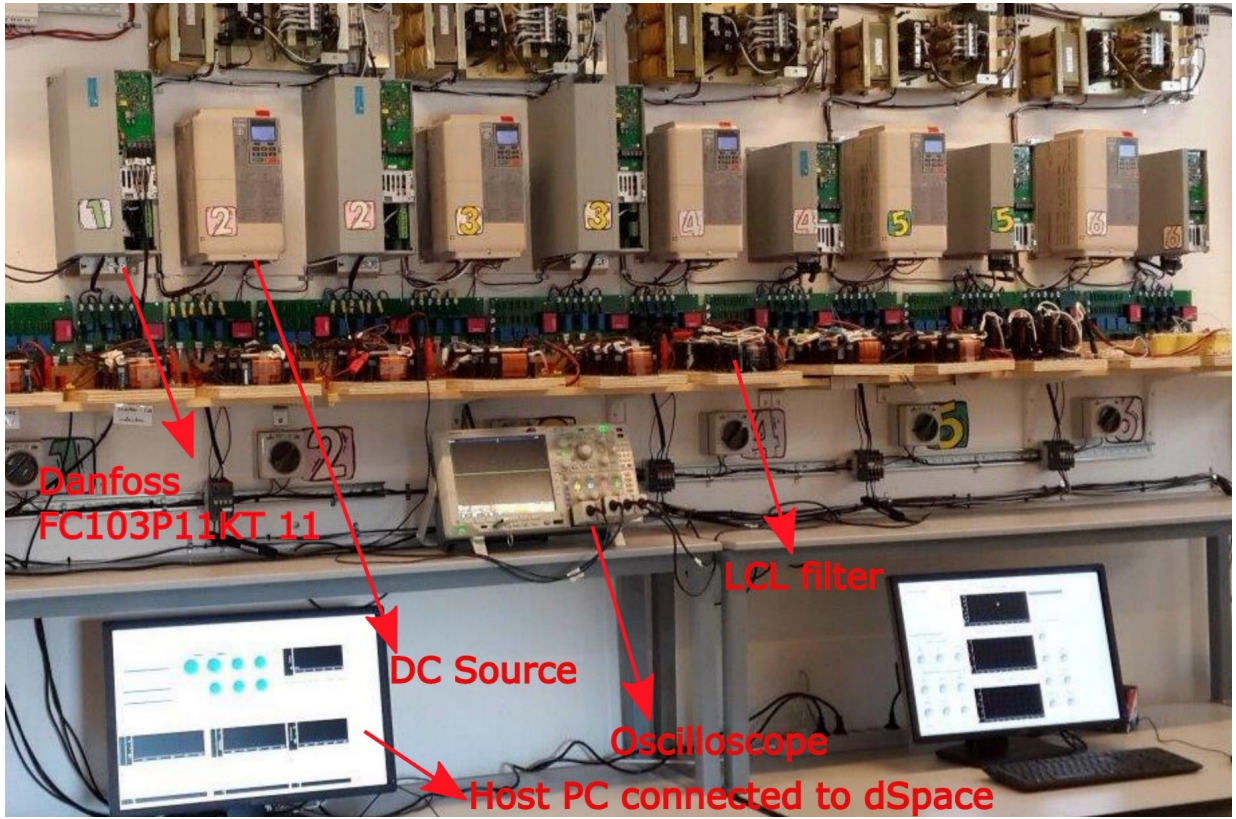

1 VSC Setup

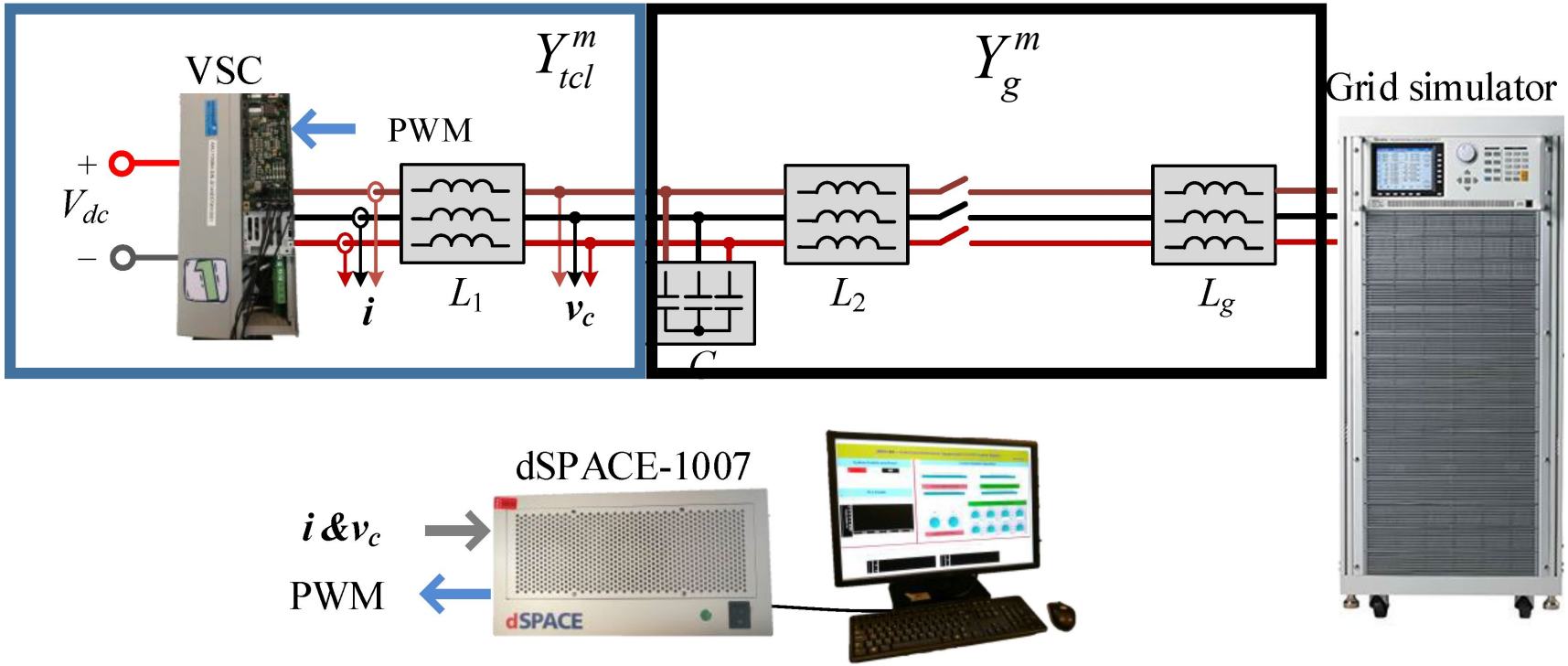
VSC
Y_{tcl}^m
PWM
+
V_{dc}
−
i
L_1
v_c
Y_g^m
L_2
L_g
C
Grid simulator
dSPACE-1007
i &v_c
PWM
dSPACE

Harmonic Stability

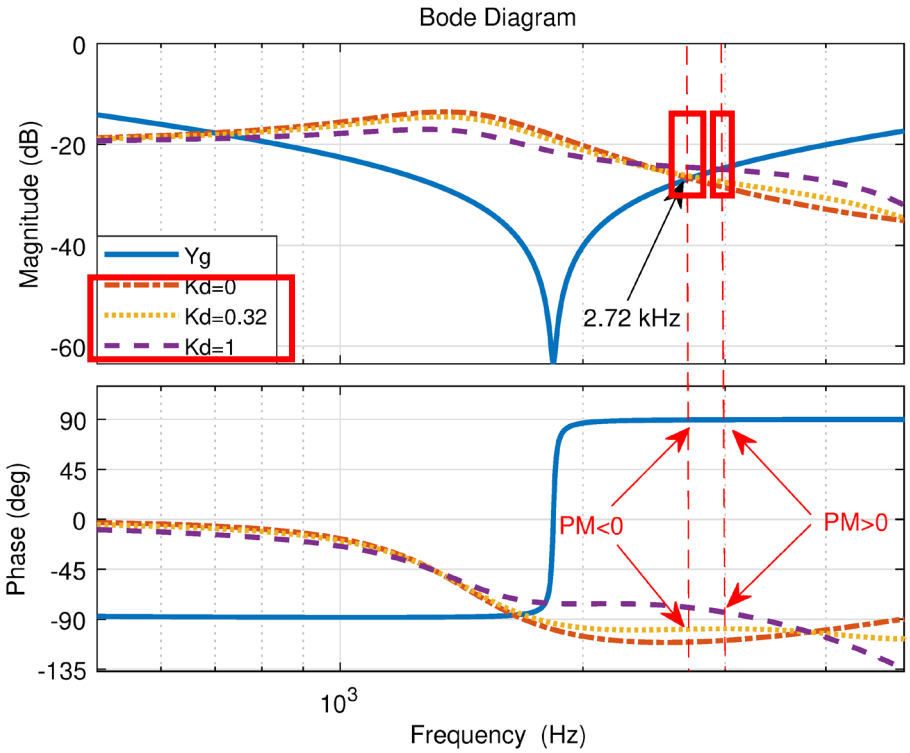

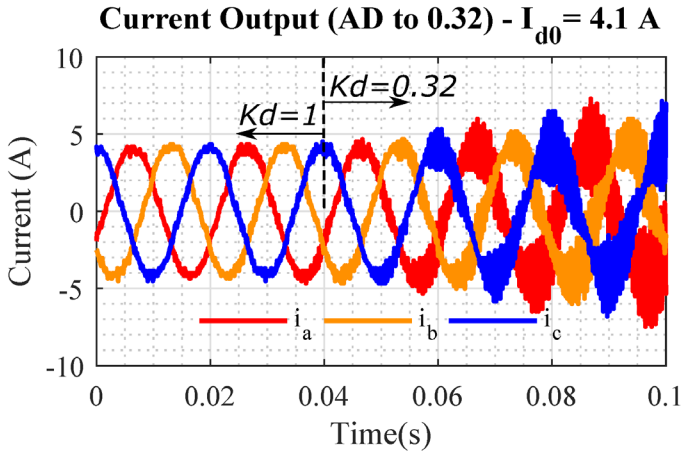

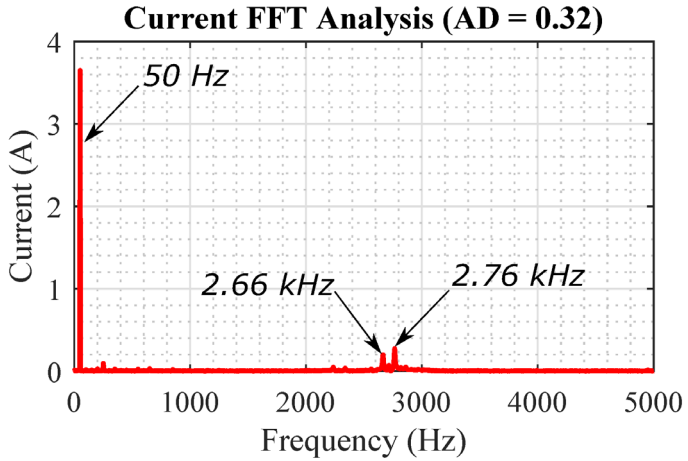

Generation Mode – I_{d0}= + 11.2 A

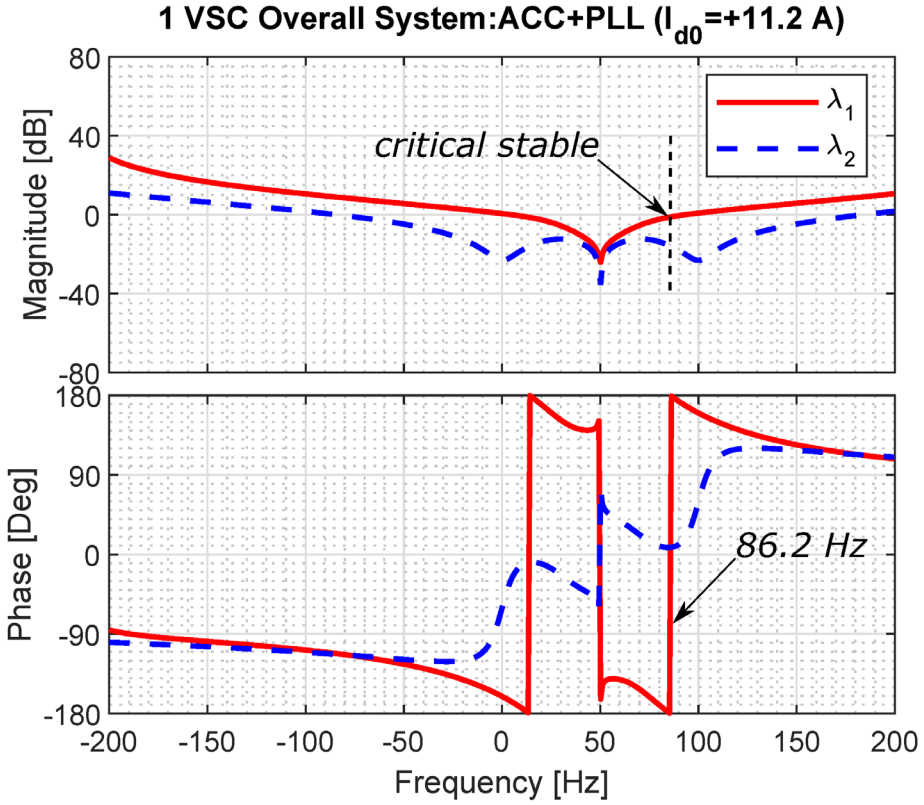

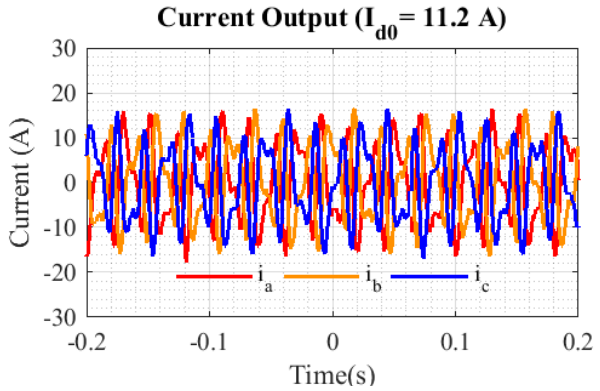

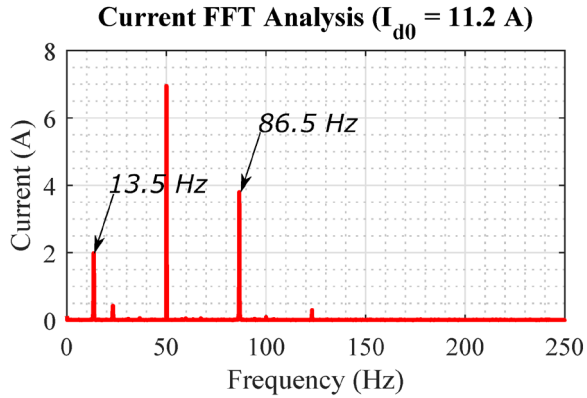

Generation Mode – I_{d0}= + 14.58 A

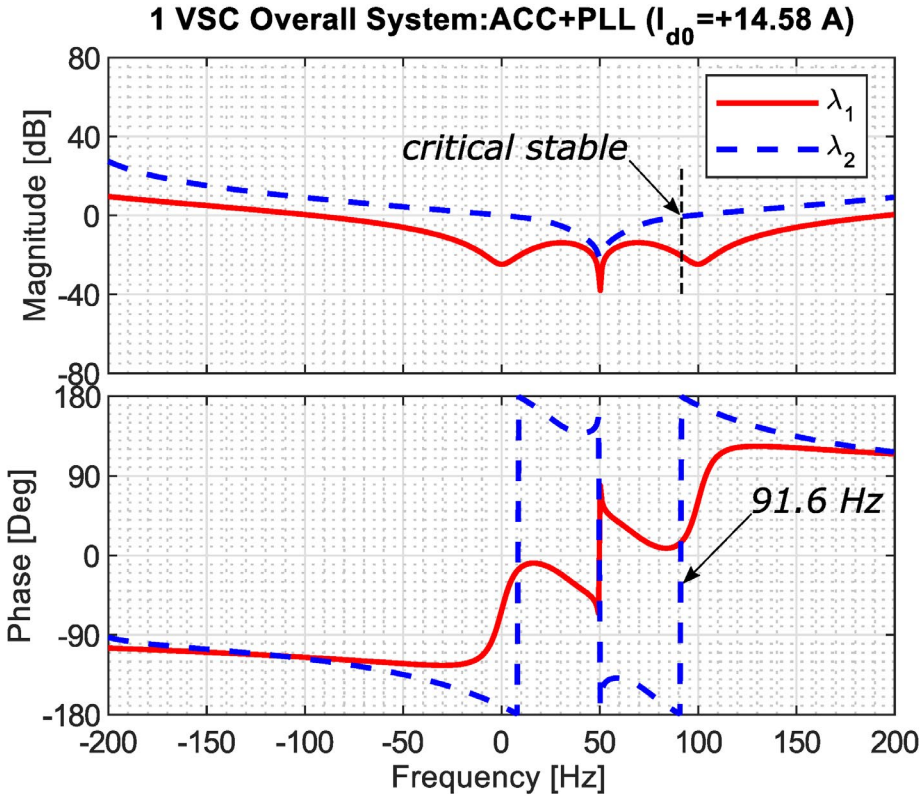

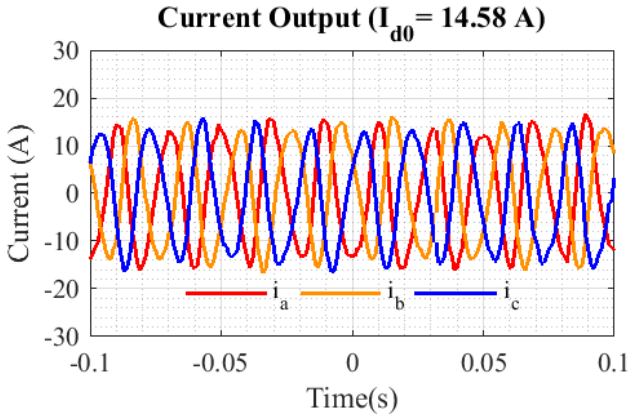

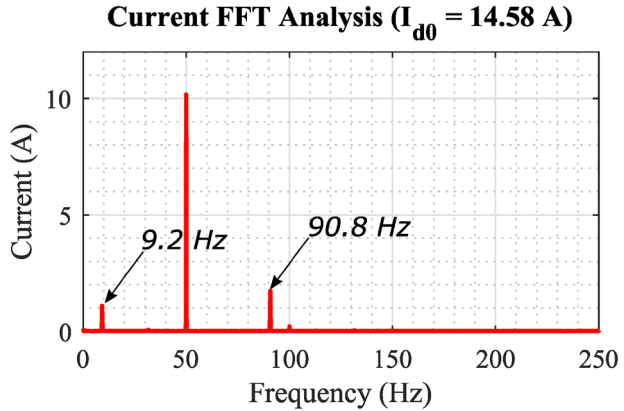

2 VSC Setup

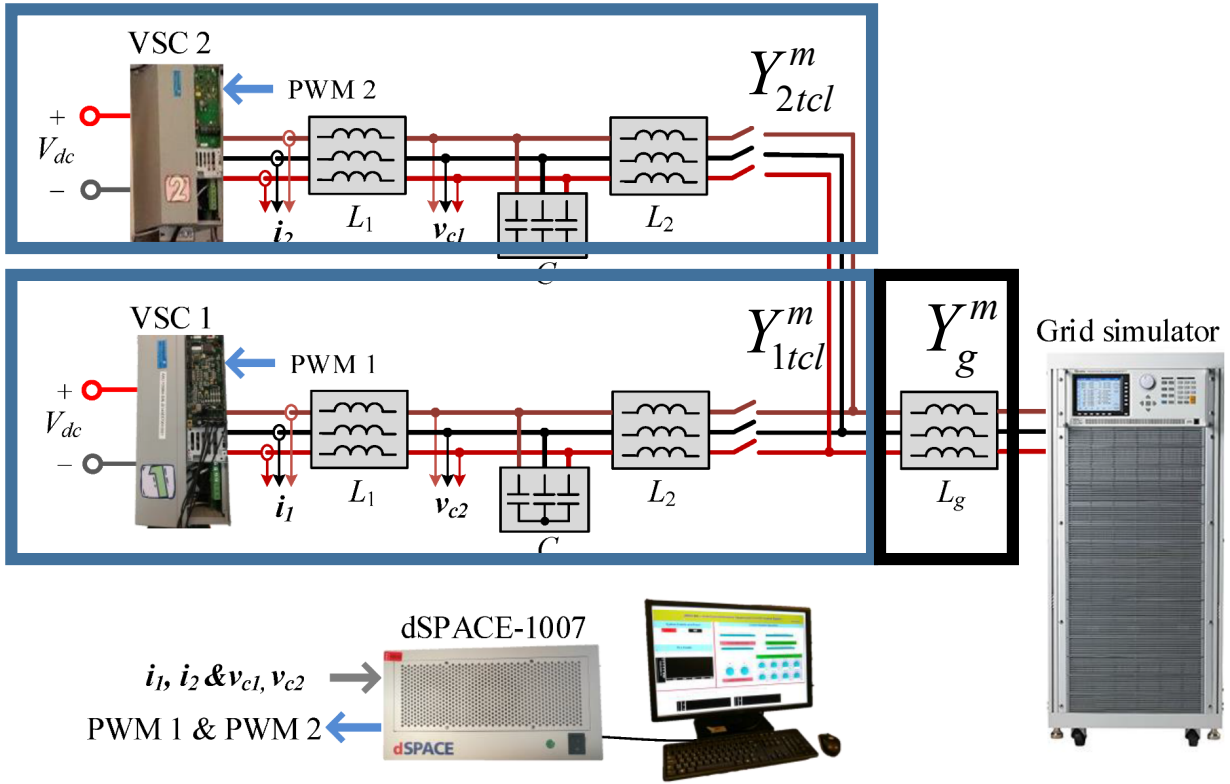
VSC 2
PWM 2
Y^m_{2tcl}
V_{dc}
i_2
L_1
v_{c1}
C
L_2
VSC 1
PWM 1
Y^m_{1tcl}
i_1
v_{c2}
Y^m_g
L_g
Grid simulator
dSPACE-1007
$i_1, i_2 \& v_{c1}, v_{c2}$
PWM 1 & PWM 2
dSPACE

2 VSC Experimental Results

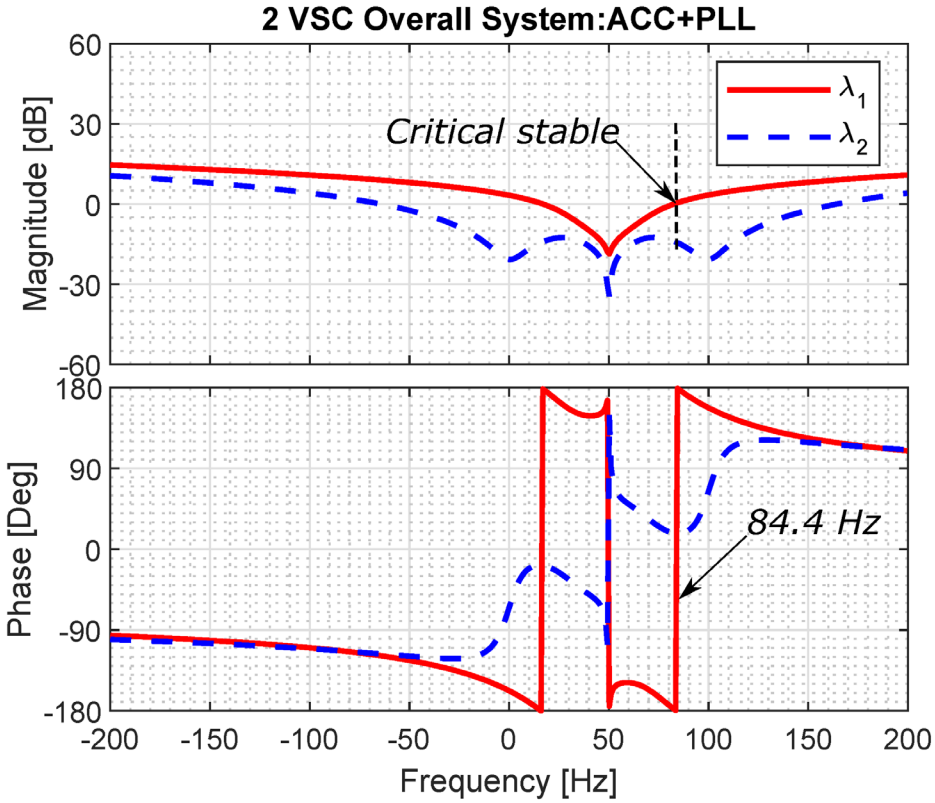

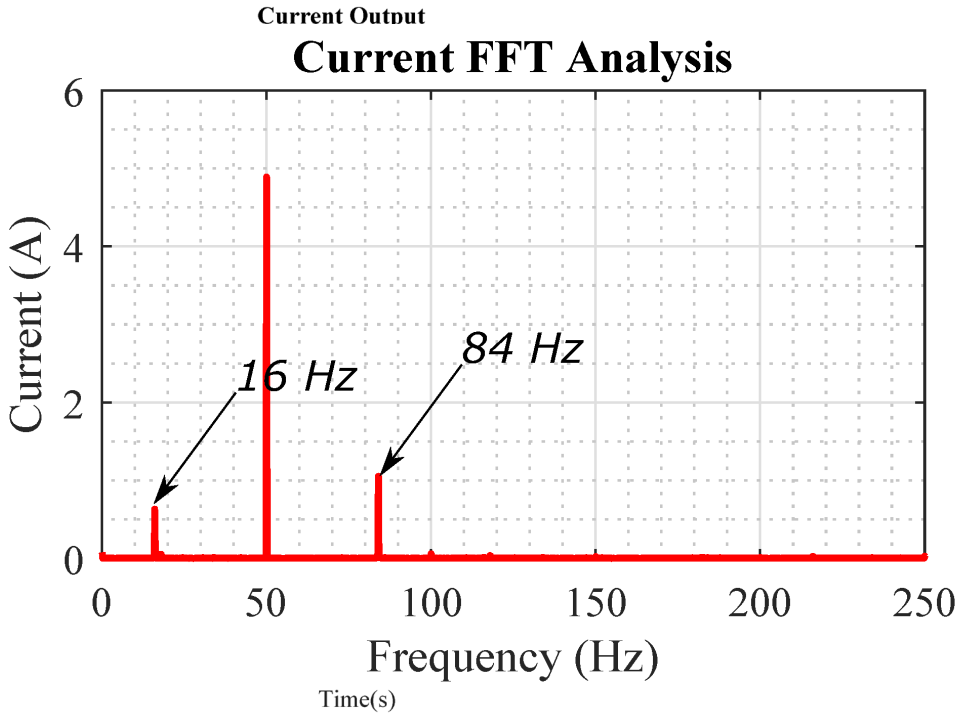

Results - Table

Tab. 5.3: Experimental validation results - Single VSC setup

VSC operating points	Analytical prediction	Experimental results	ACC parameters	PLL parameters
$I_{d0} = +11.20$ A	86.2 Hz 13.8 Hz (Fig. 5.18)	86.5 Hz 13.5 Hz (Fig. 5.19)	phase margin $\pi/4$	settling time 40 ms
$I_{d0} = +14.75$ A	91.6 Hz 8.4 Hz (Fig. 5.20)	90.8 Hz 9.2 Hz (Fig. 5.21)	phase margin $\pi/5$	settling time 40 ms
$I_{q0} = +9.00$ A	114.1 Hz 14.1 Hz (Fig. 5.22)	117.9 Hz 17.9 Hz (Fig. 5.23)	phase margin $\pi/4$	settling time 20 ms
$I_{q0} = +11.75$ A	127.6 Hz 27.6 Hz (Fig. 5.24)	127.4 Hz 27.4 Hz (Fig. 5.25)	phase margin $\pi/5$	settling time 20 ms
$I_{q0} = -9.00$ A	50 Hz (Fig. 5.26)	50 Hz (Fig. 5.27)	phase margin $\pi/4$	settling time 20 ms

Tab. 5.5: Experimental validation results - double VSC setup

VSC operating points	Analytical prediction	Experimental results	ACC parameters	PLL parameters
$I_{1d0} = +7.00$ A $I_{2d0} = +1.85$ A	84.4 Hz 15.6 Hz (Fig. 5.29)	84.0 Hz 16.0 Hz (Fig. 5.30)	phase margin $\pi/5$	settling time 40 ms
$I_{1q0} = +5.00$ A $I_{2q0} = +1.55$ A	105.1 Hz 5.1 Hz (Fig. 5.31)	110.0 Hz 10.0 Hz (Fig. 5.32)	phase margin $\pi/5$	settling time 20 ms
$I_{1q0} = +8.00$ A $I_{2q0} = +5.45$ A	90.7 Hz 9.3 Hz (Fig. 5.33)	91.6 Hz 8.4 Hz (Fig. 5.34)	phase margin $\pi/5$	settling time 40 ms

- PLL controller impact
- Setpoint dependent impact
- ACC controller impact

Summary

- The grid-connected VSC can cause small-signal voltage instability when its digital delay is adversely interacting with the impedance resonance point formulated by LCL filter and the equivalent grid impedance.
- Active damping is an effective method to improve the phase margin of the small-signal voltage stability
- The PLL of the grid-connected VSC is identified as dominant contributor to the small-signal voltage instability phenomena.
- The increased penetration level of the two-level VSC connected renewable generation can lead to the small-signal voltage instability.
- Increasing ACC controller bandwidth of the VSC can improve overall voltage stability